Available online www.jocpr.com

Journal of Chemical and Pharmaceutical Research, 2012, 4(7):3400-3413

Research Article

ISSN : 0975-7384
CODEN(USA) : JCPRC5

Vibrational spectra and electrostatic potential surface of 2-fluoro-6-methoxybenzonitrile based on quantum chemical calculations

M. Murugan[a], V. Balachandran[a*] and M. Karnan[b]

[a]*PG & Research Department of Physics, A A Government Arts College, Musiri, Tiruchirappalli 621 211, India*
[b]*Department of Physics, Srimad Andavan Arts and Science College, Tiruchirappalli 620 005, India*

ABSTRACT

In this work, the experimental and theoretical study on molecular structure and vibrational spectra of 2-fluoro-6-methoxybenzonitrile (FMBN) are studied. The FT-Raman and FT-IR spectra of FMBN were recorded. Geometrical parameters and vibrational wavenumbers are calculated using ab initio Hartree-Fock (HF) and Density Functional Theory (DFT) levels employing the 6-31G(d,p) basis set. Comparison of the simulated spectra provides important information about the ability of the computational method (B3LYP) to describe the vibrational modes. The complete assignments are performed on the basis of the total energy distribution (TED). The molecular stability and bond strength were investigated by applying the Natural Bond Orbital (NBO) analysis. The calculated HOMO and LUMO energies show that charge transfer occur in the molecule. Information about the size, shape, charge density distribution and site on chemical reactivity of the molecule was obtained by mapping electron density isosurface with Electrostatic Potential (ESP).

Keywords: HF, DFT, Vibrational spectra, 2-fluoro-6-methoxybenzonitrile, HOMO-LUMO, NBO.

INTRODUCTION

Benzonitrile (BN) is a phenyl cyanide compound which is derived mainly from benzoic acid reaction with lead thiocyanate by heating. It reacts violently with strong acids to produce toxic hydrogen cyanide and it decomposes on heating, producing very toxic fumes of hydrogen cyanide and nitrous oxides [1]. Several benzonitrile derivatives have important applications and the importance of these compounds has been reviewed [2]. Benzonitrile is used as a solvent and chemical intermediate for the synthesis of pharmaceuticals, dye stuffs and rubber chemicals through the reactions of alkylation, condensation, esteerification, hydrolysis, halogenation or nitration. Benzonitrile and its derivatives are used in the manufacturing of lacquers, polymers and anhydrous metallic salts as well as intermediates for pharmaceuticals, agrochemicals and other organic chemicals. Many derivatives of benzonitrile are used in medicine as urinary antiseptic in the form of salt and in vapour form for disinfecting bronchisl tubes. They are also used in dye industry for making aniline blue and for preserving food products [3].

Vibrational wavenumbers and thermodynamic parameters for the 3,5-difluorobenzonitrles using *ab initio* quantum chemical methods have been reported by Rastogi *et al.* [4]. Virendra Kumar *et al.* [5] have reported FT-IR and FT-Raman spectra of 2-chloro-6-methylbenzonitrile by *ab initio* HF levels. The F and Cl monosubstituted BN derivatives have been investigated by vibrational spectroscopy [6, 7]. Vibrational spectra of the 4-aminobenzonitrile have been studied by applying the HF and DFT levels of theory by Alcolea Palafox *et al.* [8]. Chloro-disubstituted [9] BN and chloro and methyl–disubstituted [10–12] BNs have been studied by infrared spectroscopy. Vibrational assignments, atomic charges, several therodynamic parameters and dipole moments of some di-substituted benzonitriles have been reported [4,13]. Experimental infrared and Raman spectra, vibrational assignment and normal coordinate analysis of 2,3,4-, 2,3,6-, 2,4,5- and 3,4,5-tri-fluorobenzonitriles have been reported by Mukherjee et al [14]. But, to our knowledge, no structural data obtained either by experimental or theoretical methods have been reported so far for

the title compound, FMBN. Especially, there have been no reports on the bioactivities of this compound till now, so we have concentrated on the title compound and determination of its bioactivities are currently in the progress. On the other hand, in recent years, quantum chemical calculations have become an increasingly useful tool for experimental studies. The success of DFT levels is mainly due to the fact that it describes small molecules more reliably than Hartree-Fock theory. It is also computationally less demanding than wave function based methods with inclusion of electron correlation [15,16]. Thus, in order to characterize the correlation between molecular structure and macroscopic properties in the studied compound, it seems to be essential to undertake a detailed comparative study of the isolated molecule and the solid state unit. In this paper, a concerted approach by *ab initio* and DFT levels were used, which takes advantage of the high interpretative power of the theoretical studies and the precision and reliability of the experimental data. At the same time, a comparison of some geometrical parameters are also made with those of a similar compound 3-fluoro-(4-hydroxyphenoxy) benzonitrile which was reported by Zheng *et al*. [17]. Furthermore, we have attempted to study the HOMO-LUMO and NBO analysis of FMBN using B3LYP level of theory with the standard 6–31+G(d,p) basis set implemented in the Gaussian 09 [18] program. Geometries obtained from DFT levels were used to perform NBO analysis.

EXPERIMENTAL SECTION

The compound FMBN was provided by Lancaster Chemical Company, UK, and it was used as such without further purification. The FT-IR spectrum of FMBN was recorded at room temperature in the region 4000–400 cm^{-1} using Perkin-Elmer spectrum RX1 spectrophotometer equipped with KBr pellet technique. The signals were collected for 100 scans with a scan interval of 1 cm^{-1} and at optical resolution of 0.4 cm^{-1}. The FT-Raman Nexus 670 spectrometer was used for the Raman spectral measurements at room temperature. The spectrometer consisted of a quartz beam splitter and a high sensitive germanium diode detector cooled to the liquid nitrogen temperature. The samples were packed in a glass tube of about 5 mm diameter and excited in the 180° geometry with 1064 nm laser line at 75 mW power from a diode pumped air cooled-cw Nd:YAG laser as excitation wavelength in the region 3500–100 cm^{-1}. The signals were collected for 300 scans at the interval of 1 cm^{-1} and optical resolution of 0.1 cm^{-1}.

COMPUTATIONAL DETAILS

The optimized structural parameters were used in the vibrational wavenumber calculation at the *ab initio* HF [19] DFT level at the B3LYP (Becke-3-Lee-Yang-Parr three parameters) hybrid functional with correlation function such one proposed by Lee, Yang and Parr [20, 21]. B3LYP is most promising in providing reasonably acceptable vibrational wavenumbers for organic molecules. As a result, the unscaled calculated wavenumbers, reduced masses, force constants, infrared intensities, Raman activities, and depolarization ratios are obtained. In order to fit the theoretical wavenumbers to the experimental, the scaling factors have been introduced by using a least square optimization method. Vibrational frequencies calculated at HF/6-31G(d,p) and B3LYP/6-31G(d,p) levels were scaled by 0.9981 above 1700 cm^{-1} and 0.8863 below 1700 cm^{-1} [22]. Standard 6-31G(d,p) basis set has been used in both levels in order to see the effect of correlation. Gaussian 09 software package [18] and the levels implemented therein have been utilized to accomplish all the calculation. The Cartesian representation of the theoretical force constants have been computed at the fully optimized geometry by assuming the molecule belongs to Cs point group symmetry. The transformation of force field and the subsequent normal coordinate analysis (NCA) including the least-squares refinement of the scaling factors, calculations of the potential energy distribution (TED), and the prediction of IR and Raman intensities were done on a PC with the MOLVIB program (7.0- G77) written by Tom Sundius [23]. From the basic theory of Raman scattering, Raman activities (S_i) calculated by Gaussian 09 program has been converted to relative Raman intensities (I_i) using the following relationship:

$$I_i = \frac{f(\upsilon_0 - \upsilon_i)^4 s_i}{\upsilon_i[1-\exp(-hc\upsilon_i / kT)]} \qquad \text{---------- (1)}$$

where v_0 is the laser exciting frequency in cm^{-1} (in this work, we have used the excitation wavenumber ν_0=9398.5 cm^{-1}, which corresponds to the wavelength of 1064 nm of a Nd:YAG laser), v_i is the vibrational wavenumber of the *i th* normal mode (in cm^{-1}) and S_{Ra} is the Raman scattering activity of the normal mode v_i, f (is the constant equal to 10^{-12}) is the suitably chosen common normalization factor for all peak intensities. *h*, *k*, *c*, and *T* are Planck constant, Boltzmann constant, speed of light, and temperature in Kelvin, respectively.

A detailed description of vibrational modes can be given by means of normal coordinate analysis, for this purpose the full set of 60 standard internal coordinates (containing 15 redundancies) for the title compound is listed in Table 1. From these, a non-redundant set of local symmetry coordinates was constructed by suitable linear combinations of

internal coordinates following the recommendations of Pulay and Fogarasi [24, 25] which are given in Table 2. The theoretically calculated DFT force fields were transformed to this set of vibrational coordinates and used in all subsequent calculations.

Natural bond orbital analysis was performed by the Gaussian program at the B3LYP level of theory analysis transforms the canonical delocalized Hartee Fock (HF) *MOs* into localized orbital's that are closely tied to chemical bonding concepts. This process involves sequential transformation of non orthogonal Atomic Orbital's (*AOs*) to the sets of Natural Atomic Orbital's (*NAOs*), Natural Hybrid Orbital's (*NHOs*) and NBOs. Natural bond orbital analysis gives the accurate possible natural Lewis structure picture of orbital because all orbitals are mathematically chosen to include the highest possible percentage of the electron density. Interaction between both filled and virtual orbital spaces information correctly explained by the NBO analysis, it could enhance the analysis of intra and inter–molecular interactions. The interaction between filled and antibonding orbital's represent the deviation of the molecule from the Lewis structure and can be used as the measure of delocalization. This noncovalent bonding–antibonding interaction can be quantitatively described in terms of the second order perturbation interaction energy $E^{(2)}$ [26–29]. This energy represents the estimate of the off–diagonal NBO Fock Matrix elements. It can be deduced from the second – order perturbation approach [30];

$$E^{(2)} = \Delta E_{ij} = q_i \frac{F^2_{(1,2)}}{\varepsilon_j - \varepsilon_i} \qquad \text{... (2)}$$

where q_i is the i^{th} donor orbital occupancy, $\varepsilon_j, \varepsilon_i$ the diagonal elements (orbital energies) and F (j,i) the off diagonal NBO Fock Matrix element.

Table 1 Definition of internal coordinates of 2-fluro-6-methoxybenzonitrile

No(i)	Symbol	Type	Definition[a]
Stretching			
1-3	r_i	C–H (Aromatic)	C_5-H_{12}, C_4-H_{11},C_3-H_{10}
4-5	q_i	C–O	C_6-O_{13}, O_{13}-C_{14}
6	s_i	C–F	C_2-F_9
7	t_i	C–N (Nitrile)	C_7-N_8
8-13	p_i	C–C (Aromatic)	C_1-C_2, C_2-C_3, C_3-C_4, C_4-C_5,C_5-C_6, C_6-C_1
14	T_i	C–C	C_1-C_7
15-17	R_i	C–H (Methyl)	C_{14}-H_{15}, C_{14}-H_{16}, C_{14}-H_{17}
18-23	α_i	C–C–C	C_1-C_2-C_3, C_2-C_3-C_4, C_3-C_4-C_5, C_4-C_5-C_6, C_5-C_6-C_1, C_6-C_1-C_2
In-plane bending			
24-29	β_i	C–C–H	C_2-C_3-H_{10}, C_4-C_3-H_{10}, C_3-C_4-H_{11}, C_5-C_4-H_{11}, C_4-C_5-H_{12}, C_6-C_5-H_{12}
30,31	γ_i	C–C–F	C_1-C_2-F_9, C_3-C_2-F_9
32,33	θ_i	C–C–O	C_5-C_6-O_{13}, C_1-C_6-O_{13}
34,35	π_i	C–C-C	C_6-C_1-C_7, C_2-C_1-C_7
36	ψ_i	C–C–N	C_1-C_7-N_8
37	ϕ_i	C–O–C	C_6-O_{13}-C_{14}
38-40	σ_i	O–C–H	O_{13}-C_{14}-H_{15}, O_{13}-C_{14}-H_{16}, O_{13}-C_{14}-H_{18}
41-43	e_i	H–C–H	H_{15}-C_{14}-H_{17}, H_{17}-C_{14}-H_{16}, H_{16}-C_{14}-H_{15}
Out-of-plane bending			
44-49	ω_i	C-C-C-C (ring)	C_1-C_2-C_3-C_4, C_2-C_3-C_4-C_5, C_3-C_4-C_5-C_6, C_4-C_5-C_6-C_1, C_5-C_6-C_1-C_2, C_6-C_1-C_2-C_3
50	ω_i	C-C-C-F	F_9-C_2-C_1-C_3
51	ω_i	C-C-C-C	C_6-C_1-C_7-C_2
52,53	ω_i	C-C-C-N	C_6-C_1-C_7-N_8, C_2-C_1-C_7-N_8
54	ω_i	C-C-C-O	O_{13}-C_6-C_1-C_5
55-57	ω_i	C-C-C-H	H_{10}-C_3-C_2-C_4, H_{11}-C_4-C_5-C_3, H_{12}-C_5-C_4-C_6
58-60	ω_i	C-O-C-H	C_6-O_{13}-C_{14}-(H_{15},H_{16},H_{17},

[a] *For numbering of atoms refer Fig.1*

Table 2 Definition of local symmetry coordinates of 2-fluro-6-methoxybenzonitrile

No	Type	Definition[a]
1-3	C-H	r_1, r_2, r_3
4,5	C-O	q_4, q_5
6	C-F	s_6
7	C-N	t_7
8-13	C-C	p_8, p_9, p_{10}, p_{11}, p_{12}, p_{13}
14	C-C	T_{14}
15	CH3 ss	$(R_{15} + R_{16} + R_{17})/\sqrt{3}$
16	CH3 ips	$(2R_{15} - R_{16} - R_{17})/\sqrt{6}$
17	CH3 ops	$(R_{16} - R_{17})/\sqrt{2}$
18	R trigd	$(\alpha_{18} - \alpha_{19} + \alpha_{20} - \alpha_{21} + \alpha_{22} - \alpha_{23})/\sqrt{6}$
19	R symd	$(-\alpha_{18} - \alpha_{19} + 2\alpha_{20} - \alpha_{21} - \alpha_{22} + 2\alpha_{23})/\sqrt{6}$
20	R asymd	$(\alpha_{18} - \alpha_{19} + \alpha_{21} - \alpha_{22})/2$
21 - 23	bCH	$(\beta_{24} - \beta_{25})/\sqrt{2}$, $(\beta_{26} - \beta_{27})/\sqrt{2}$, $(\beta_{28} - \beta_{29})/\sqrt{2}$
24	bCF	$(\gamma_{30} - \gamma_{31})/\sqrt{2}$
25	bCO	$(\theta_{32} - \theta_{33})/\sqrt{2}$
26	bCC	$(\pi_{34} - \pi_{35})/\sqrt{2}$
27	bCN	ψ_{34}, ψ_{35}, ψ_{36}
28	bCO	ϕ_{37}
29	CH_3 sb	$(-\rho_{38} - \rho_{39} - \rho_{40} + \sigma_{41} + \sigma_{42} + \sigma_{43})/\sqrt{6}$
30	CH_3 ipb	$(-\sigma_{41} - \sigma_{42} + 2\sigma_{43})/\sqrt{6}$
31	CH_3 opb	$(\sigma_{41} - \sigma_{42})/\sqrt{2}$
32	CH_3 ipr	$(2\rho_{38} - \rho_{39} - \rho_{40})/\sqrt{6}$
33	CH_3 opr	$(\rho_{39} - \rho_{40})/\sqrt{2}$
34	ωRtrigd	$(\tau_{44} + \tau_{45} + \tau_{46} + \tau_{47} + \tau_{48} + \tau_{49})/\sqrt{6}$
35	ω Rsymd	$(\tau_{44} + \tau_{46} + \tau_{48} + \tau_{49})/2$
36	ω Rasymd	$(-\tau_{44} + 2\tau_{45} - \tau_{46} + \tau_{47} + 2\tau_{48} - \tau_{49})/\sqrt{2}$
37	ωCF	ω_{50}
38	ωCC	ω_{51}
39,40	ωCN	ω_{52}, ω_{53}
41	ωCCO	ω_{54}
42-44	ωCCCH	ω_{55}, ω_{56}, ω_{57}
45	tCH3	$(\tau_{55} + \tau_{59} + \tau_{60})$ / 3

[a] *For numbering of atoms refer Fig.1*

RESULTS AND DISCUSSION

Geometric structure

The optimized molecular structure of the FMBN belongs to Cs point group symmetry with numbering scheme is presented in Fig.1. The existences of two rotational isomers (O-cis and O-trans) in FMBN have been demonstrated. The energy values of *cis* and *trans* for FMBN by HF/6-31G(d,p) and B3LYP/6-31G(d,p) are given in Table 3. It has further been shown that *O-trans* isomer is more stable. The optimized bond lengths and angles are calculated using HF/6-31G(d,p) and B3LYP/6-31G(d,p) levels of theory. Calculated geometrical parameters are given in Table 4. The optimized structure of the title compound was compared with other similar systems for which the crystal structures have been solved [31]. Therefore optimized geometrical parameters of 3-fluoro-(4-hydroxyphenoxy) benzonitrile [17] are compared to those of title compound. Since all the carbon atoms in the benzene ring are sp^2 hybridized and having equal bond lengths and bond angles. Hence, substitution of hydrogen in benzene ring results in the perturbation of the valence electron distribution of the molecule followed by changes in the various chemical and

physical properties. The angular changes in benzene ring geometry have proved to be a sensitive indicator of the interaction between the substituents and the benzene ring [32]. The bond lengths in the ring have also shown characteristic variation but they have been small and less well pronounced as compared to the angular changes. All calculated bond lengths and experimental data are given in Table 4. The experimental C–C bond lengths of the aromatic ring fall in the range from 1.39 to 1.38 Å, while the results obtained from the HF and B3LYP levels fall in the range 1.38 to 1.40 for title molecule. In this table, the bond lengths of aromatic ring carbon atom are C1–C2, C1–C6, C2–C3, C3–C4, C4–C5 and C5–C6 for 1.39, 1.40, 1.38, 1.39, 1.38, 1.38 Å and 1.40, 1.42, 1.39, 1.39, 1.39, 1.39 Å obtained by HF/631-G(d,p) and B3LYP/6-31G(d,p), levels theory and their corresponding experimental values are 1.39, 1.38, 1.38, 1.38 Å for C2–C5, C3–C4, C4–C5 and C5–C6, respectively.

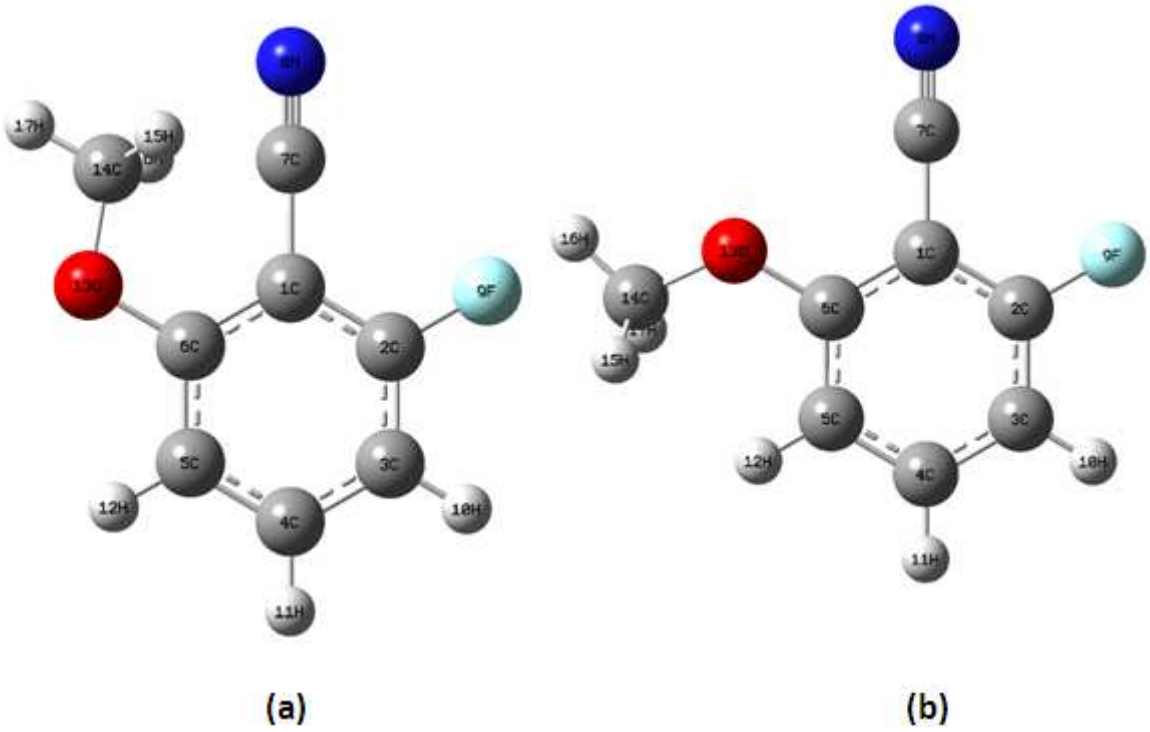

Fig. 1 Optimized molecular structure of 2-fluoro-6-methoxybenzonitrile

Table 3 Global minimum energy of 2-fluro-6-methoxybenzonitrile based on HF/6-31G(d,p) and B3LYP/6-31G(d,p)

Conformer	HF/6-31G(d,p)		B3LYP/6-31G(d,p)	
	In hartrees	In kJ/mol	In hartrees	In kJ/mol
O-cis	–535.13701	–1405002.3268	–538.22247	–1413103.2026
O-trans	–535.14837	–1405032.1526	–538.23295	–1413130.7179
Energy difference	–0.01135	–29.826	–0.01048	–27.515

The calculated bond length of the C–CN (sp^2-sp^2) hybridization is 1.14 and 1.16 by HF and B3LYP levels of theory respectively, and the corresponding experimental value is 1.14 which is less than the calculated bond length due to the conjugation with the aromatic benzene ring. Moreover, the length of the triple bond of the nitrile group is reduced nitrile group on *para* position.

Analysis of available experimental data has to the conclusion that for many of the substituent, the angular distortion of the benzene ring can be interpreted as a superposition of the contribution of the each substituent. The structural changes on the carbon skeleton concern both the bond distances and bond angles. They are the most pronounced at the place of substitution and depend on the electronegativity as well as the σ/π donor/acceptor character of the substituent.

The increase of the C–C bond lengths adjacent to the C1–C7 bond in the substitution place is accompanied by slightly irregular hexagonal structure of the *ipso* angle C2–C1–C6, 118.6 and 118.2 at the HF/6-31G(d,p) and B3LYP/6-31G(d,p) level. This value is in accordance with that of the 118.85, 118.76 in contrast with the almost null change calculated in BN, 120.030 indicated that the C≡N along has no effect. Comparing the HF/6-31G(d) and B3LYP/6-31G(d) methods, most of the bond lengths and bond angles of HF/6-31+G(d) are slightly shorter due to the neglect of electron correlation.

Table 4 Optimized geometrical parameters of 2-fluro-6-methoxybenzonitrile

Parameters	Bond length			Parameters	Bond angles		
	HF/ 6-31G(d,p)	B3LYP/ 6-31G (d,p)	Expt[a]		HF/ 6-31G(d,p)	B3LYP/ 6-31G (d,p)	Expt[a]
C_1-C_2	1.3876	1.404		C_2 - C_1 - C_6	118.6	118.2	
C_1-C_6	1.3971	1.416		C_2 - C_1 - C_7	120.4	119.5	120.5
C_1-C_7	1.4387	1.427	1.425	C_1 - C_2 - C_3	122.2	122.5	122.8
C_2-C_3	1.3751	1.3855	1.391	C_1 - C_2 - F_9	118.4	118.0	118.7
C_2-F_9	1.3193	1.341	1.350	C_3 - C_2 - F_9	119.3	119.4	118.5
C_3-C_4	1.3853	1.395	1.379	C_2 - C_3 - C_4	118.2	118.2	118.4
C_3 - H_{10}	1.073	1.083	0.930	C_2 - C_3 - H_{10}	119.5	119.4	120.0
C_4 - C_5	1.3846	1.394	1.379	C_4 - C_3 - H_{10}	120.3	122.3	120.0
C_4 - H_{11}	1.075	1.085	0.930	C_3 - C_4 - C_5	121.2	121.0	119.9
C_5 - C_6	1.3839	1.396	1.375	C_3 - C_4 - H_{11}	119.3	119.3	119.6
C_5 - H_{12}	1.0736	1.083	0.930	C_5 - C_4 - H_{11}	119.4	119.5	119.6
C_6 - O_{13}	1.3473	1.362		C_4 - C_5 - C_6	119.7	120.3	119.5
C_7 - N_8	1.1357	1.163	1.135	C_4 - C_5 - H_{12}	121.3	121.4	120.8
$O_{13—C14}$	1.4151	1.437		C_6 - C_5 - H_{12}	118.8	118.1	120.8
C_{14} - H_{15}	1.0849	1.092		C_1 - C_6 - O_{13}	119.9	119.6	
C_{14} - H_{15}	1.0792	1.090		C_1 - C_7 - N_8	116.6	119.8	177.8
C_{16} - H_{17}	1.0833	1.096		C6 - O_{13} - H_{14}	110.6	117.5	
				O_{13} - C_{14} -H_{15}	106.2	112.0	
				O_{13}-C_{14}-H_{17}	109.7	110.4	
				H_{15}-C_{14}-H_{16}	109.7	109.2	

[a]*Taken from Ref.[17]*

Vibrational assignments

The 45 normal modes of FMBN are distributed among the symmetry species as Γ3N-6 = 31 A' (in-plane) + 14 A" (out-of-plane) by assuming Cs point group symmetry. The calculated normal modes of vibrational frequencies provide thermodynamic properties by statistical mechanics. The observed and calculated frequencies, IR intensities, Raman scattering activities and probable assignments and TED of FMBN have been reported in Table 5. The observed experimental (FT-IR and FT-Raman) and simulated (B3LYP/6-31G(d,p)) spectra are shown in Figs. 2 and 3, respectively. Some important modes of vibrations have been discussed as follows:

C–H vibrations

In higher frequency region almost all vibrations belong to C–H stretching [33, 34]. In this region, the bands are not affected appreciably by the nature of the substituent. In the present study, the bands observed at 3068, 3033, 2982 cm^{-1} in FT-IR spectrum and 3071, 3036, 2986 cm^{-1} in FT-Raman spectrum have been assigned to C–H stretching vibrations. The C–H bending vibrations are expected to interact a little around 1600 – 1300 cm^{-1} with ring vibrations [33]. Hence in the present study, the bands observed at 1318, 1258 and 1215 cm^{-1} in FT-Raman spectrum have been assigned to C–H in-plane bending modes. The bands at 701, 542 cm^{-1} in FT Raman spectrum and 674, 540 cm^{-1} in FT–IR spectrum are associated with C–H out-of-plane bending modes.

C≡N vibrations

The C≡N stretching displays itself around 2200 cm–1 which is of variable intensity on conjugation as in nitriles the frequency gets lowered and the band becomes stronger. The presence of nitriles can be detected from this band [34]. The stretching mode is highly localized on the C≡N bond with a total energy distribution of 86%. In benzonitriles [35] this vibration appears in the 2220–2240 cm–1 range, in accordance with our results, and with IR intensity which varies from medium to strong depending on the substituent. This electron withdrawing groups, as the FT–IR band intensity is slightly decreased and increased the wavenumber to the higher limit of the spectral region. In BN, this band has been identified at 2230 cm–1, we can expect that in FMBN it appears to a slightly higher wavenumber, as it is observed in Table 5 and close to that reported in difluorobenzonitrile [35, 36] at 2230 cm–1 in FT-IR spectrum and 2234 cm–1 in FT-Raman spectrum. It mixed with C–O stretching mode to the extent of 12% as in BN derivative. Successive substitution of electron-withdrawing or donating groups can also shift the C≡N stretching wavenumber beyond the characteristics wavenumber region mentioned above e.g. in 2,3,5,6-tetrafluoro-4-cyanobenzonitrile it is at 2253 cm–1. Contribution of the bending in-plane mode are determined in the bands at approximately 600, 550 and 30 cm–1 while the out-of-plane mode is identified in the infrared band at 420 cm–1, in contradiction with that reported in MFBN [37] at 606 cm–1. Hence in the present study, the C≡N in-plane and out-of-plane bending modes are recorded at 651 cm–1 in FT–IR. These bands are in good agreement with the calculated values are found at 650 and 544 cm–1, respectively.

Table 5 Observed and calculated vibrational wavenumbers (cm^{-1}), IR intensities (km/mol) and Raman scattering activities (A^4/amu) of 2-fluoro-6-methoxybenzonitrile.

Mode	Symmetry species	Observed frequency		Calculated frequency				Vibrational Assignments/TED(%)
				Unscaled		Scaled		
		FT-IR	FT-Raman	HF	B3LYP	HF	B3LYP	
1	A″			84	82	85	80	CH_3 twist (52)
2	A″			106	105	104	104	ωRtrigd (61)
3	A″		104 vw	147	141	145	142	ωRsymd (57)
4	A″		164ms	169	166	164	160	ωRasymd (62)
5	A″		193vw	221	199	198	192	ωCO (55), ωCH (16), ωCO (12)
6	A″		236vw	270	234	244	238	ωCO (55), ωCH (58), ωRsymd(12)
7	A″		302vw	326	298	306	302	ωCC (42), ωCF (20), ωCC (10)
8	A″		360vw	372	368	364	360	ωCF (46), ωCC (28), ωCH (12)
9	A'		405vw	471	415	423	407	βCC (52), ωCH (21) ωCO(10)
10	A″	423ms	457vw	486	469	452	425	ωC≡N (45), ωRtrigd (20)
11	A'		535vw	564	532	538	533	βCO(42), βCH(20), CH_3ipb(12)
12	A″	540ms	542vw	556	546	546	544	ωCH (46), ωCO (12), Rtrigd (12)
13	A'		601vw	631	609	610	606	βCO (40), βCH (22), ωCH_3opb (10)
14	A'		644ms	676	651	655	648	βC≡N (55), βCO (18), βCC (10)
15	A″	674ms		689	671	683	678s	ωCH (62)
16	A″		701ms	729	705	712	706	ωCH (66)
17	A'	785vs	787ms	831	820	800	790	βRsymd (66)
18	A'		857ms	861	871	868	861	βRasymd (68)
19	A″	875ms		905	880	888	875	CH_3opr (77), ωRtrigd (20)
20	A'		905 vw	1003	899	916	904	βCF (66)
21	A'	948vs	953 vw	1069	979	972	950	νCC (88), βCO (11)
22	A'		971ms	1028	981	995	974	νCO (86)
23	A'	1074vs	1072ms	1158	1138	1069	1069	CH_3 ipr (74) βRtrigd (21)
24	A'		1101ms	1187	1090	1096	1103	βRtrigd (62) βCC (20) νCC(10)
25	A'		1144ms	1217	1157	1145	1143	νCO (60) νCC (18) βCH (12)
26	A″		1160ms	1283	1193	1168	1150	CH_3opb (86) νCC (12)
27	A'		1186ms	1298	1210	1195	1187	CH_3sb (89) νCC (10)
28	A'		1215ms	1311	1224	1206	1211	βCH (55) νCO (25) νCC (14)
29	A'	1261s	1258ms	1325	1278	1259	1264	βCH (58), νCC (22), νCO (10)
30	A'	1295s	1311ms	1397	1331	1301	1300	νCF (80)
31	A'		1315ms	1455	1340	1350	1317	βCH (62), νCC (20), βRsymd (12)
32	A'		1386ms	1604	1475	1396	1383	CH_3 ipb (83) νCC (12)
33	A'		1457 ms	1627	1532	1518	1455	νCC (66), βCH (20), βCO (11)
34	A'	1497vs	1498 ms	1635	1536	1532	1497	νCC (65), βCH (21), νCF (10)
35	A'		1560 vw	1641	1568	1562	1560	νCC (62), βCH (22)
36	A'	1591vs	1582 ms	1656	1604	1581	1580	νCC (66), βCH (21), βRsymd (11)
37	A'	1635s	1640ms	1681	1643	1644	1638	νCC (66), βCH (22)
38	A'		1658s	1813	1793	1681	1651	νCC (67), βCH (21)
39	A'	2230s	2234vs	2372	2250	2236	2229	νCN (87), νCO (12)
40	A'	2878w	2879ms	3196	3041	2896	2875	$\nu_{ss}CH_3$ (89)
41	A'	2948w	2949ms	3272	3126	2955	2944	ν_{ass} CH_3 (97)
42	A″	2955w	2959ms	3321	3165	2962	2953	ν_{ass} CH_3 (98)
43	A'	2982w	2986ms	3365	3203	2990	2882	νCH (96)
44	A'	3033w	3036ms	3388	3226	3034	3031	νCH (98)
45	A'	3068w	3071ms	3397	3333	3072	3070	νCH (99)

s : strong; vs : very strong; ms : medium strong; w : weak; vw : very weak; ν: strctching; ass : asymetric stretching; ss : symmetric stretching; β : in-plane bending; ipb : in-plane bending; opb : out-of-plane bending; sb : symmetric bending; ipr : in-plane rocking; opr : out-of-plane rocking; R : ring; symd : symmetric deformation; asymd : asymmetric deformation; ω : out-of-plane bending; trigd : trigonal deformation.

CH_3 vibrations

The title molecule FMBN under consideration possesses only one CH_3 group. For the assignments of CH_3 group frequencies, one can expect nine fundamentals can be associated to each CH_3 group, namely the symmetrical stretching in CH_3 (CH_3 sym. stretch) and asymmetrical stretching (CH_3 asym. stretch), in-plane stretching modes (i.e, in-plane hydrogen stretching mode); the symmetrical (CH_3 sym. deform) and asymmetrical (CH_3 asy. deform) deformation modes; the in-plane rocking (CH_3 ipr), out-of-plane rocking (CH_3 opr) and twisting (tCH_3) modes. Methyl groups are generally referred as electron donating substitution in the aromatic ring system. The C–H stretching vibrations of the methyl group lie in the region 2975–2840 cm^{-1} [38, 39]. There are two strong bands around 2960 cm^{-1} and a strong band at 2870 cm^{-1} corresponding to asymmetric and symmetric stretching modes, respectively [38, 39]. In FMBN, weak FT-IR bands at 2955 (TED 98%), 2948 cm^{-1} (TED 98%) with its corresponding medium strong FT-Raman bands at 2959 and 2949 cm^{-1} are all assigned to CH_3 asymmetric stretching vibrations. Similarly, a weak FT-IR bands at 2878 cm^{-1} (TED 89%) with a medium FT-Raman band at 2879 cm^{-1} are assigned to CH_3 symmetric stretching vibrations. Of CH_3 deformation frequencies [40, 41], there are

two asymmetric bending vibrations observed in the region 1470−1420 cm^{-1} and a symmetric bending vibration near 1360 cm^{-1}. Hence, in the present investigation, the medium strong FT-Raman bands at 1386 cm^{-1} (TED 83%) and 1186 cm^{-1} (TED 89%) have been assigned to in-plane deformation and symmetric deformation with major contribution to νCC of CH_3group. These fundamentals are good agreement with the calculated values at 1396, 1195 cm^{-1} and 1383, 1187 cm^{-1} by HF/6-31G(d,p) and B3LYP/6-31G(d,p) levels respectively. The symmetric deformation vibration is generally observed to be FT-IR and FT-Raman spectra in the range 1390−1370 cm^{-1} [42]. Likewise, a medium strong FT-Raman band observed at 1186 cm^{-1} (TED 86%) with mixed contribution to the νCC, with no FT-IR band observed in FMBN molecule have been assigned to out-of-plane deformation. Thus, we have found that the vibrational bands corresponding to methyl vibrations practically remain the same in magnitude and intensity. Methyl rocking frequencies are mass sensitive and variable in position due to the interaction with skeletal stretching modes [41]. Normally, these bands are observed weakly in the range 1120−1050 cm^{-1} and 900−800 cm^{-1} [42, 44]. For the FMBN, only a very strong FT-IR band at 1074 cm^{-1} (TED 74%) combined with computed ones have been assigned, since the medium FT-IR band at 875 cm^{-1} (TED 77%) with significant contribution to the βRtrigd and Rtrigd, which have been assigned to in-plane rocking and out-of-plane rocking modes, respectively. As CH_3 twisting mode is expected below 400 cm^{-1}, the computed bands at 85 cm^{-1} and 80 cm^{-1} by HF/6-31G(d,p) and B3LYP/6-31G(d,p) methods without support by PEDs, are assigned to this mode, for no spectral measurements were possible in the region due to instrumental limits.

C–C vibrations

The ring carbon-carbon stretching vibrations occur in the region 1625−1430 cm^{-1}. For aromatic six member rings, e.g., benzene and pyridines, there are two or three bands in this region due to skeletal vibrations, the strongest usually being at about 1500 cm^{-1}. In the case where the ring is conjugated further band at about 1580 cm^{-1} is also observed. In general, the bands are of variable intensity and are observed in the regions 1625−1590, 1590−1575, 1525−1470 and 1465−1430 cm^{-1}. For the substituted benzenes with identical atoms or groups on all para-pair of ring carbon atoms, the vibrations causing the bands at 1625−1590 cm^{-1} are infrared-inactive due to symmetry considerations the compound having a centre of symmetry at the ring centre. If the groups on a para-pair of carbon atoms are different them there is no centre of symmetry and vibrations are infrared active. Based on the above literature data, in our present study the medium and strong bands observed at 1593, 1504, 1449, 1171 cm^{-1} in FT-IR spectrum and 1640, 1315 cm^{-1} in FT Raman spectrum are assigned to C–C stretching vibrations. The theoretical values by B3LYP/6-31G (d,p) level show satisfactory agreement with recorded spectral data.

In our title molecule, there are six equivalent C–C bonds in the ring1 possesses six C–C stretching vibrations. However, due to high symmetry of benzene, many modes of vibrations are infrared inactive. In general, the bands around 1650 to 1350 cm^{-1} for benzene derivatives are assigned to skeletal stretching C–C bands[45]. The bands observed at 1432, 1594 cm^{-1} in FT-IR spectrum and 1609, 1582, 1468, 1433 in FT-Raman spectrum is identified as C–C stretching vibrations. The theoretically predicted C–C stretching vibrations by B3LYP/6-31G(d,p) method are 1647, 1625, 1496, 1484 cm^{-1} corresponding to the (mode no: 10,11,13,14) as listed in Table 5. The C–C aromatic stretch known as semi circle stretching observed at 1609 cm^{-1} in FT-Raman spectrum and 1594 cm^{-1} in FT-IR spectrum.

C–F vibrations

The vibration belonging to the bond between the ring and halogen atoms is worth to discuss here, since mixing of the vibrations is possible due to the lowering of the molecular symmetry and the presence of heavy atom on the periphery of the molecule [39]. Krishnakumar *et al.* [46] assigned vibrations of C−X group (X=F, Cl and Br) in the frequency range 1292−485 cm^{-1}. Based on the above literature values band observed at 800 cm^{-1} in FT-IR spectrum is assigned to C−F stretching vibration, which highly coupled with C−C−C in-plane deformation. The theoretically computed values are found at 843 and, 818 cm^{-1} by B3LYP/6-31G(d,p) method show good agreement with recorded spectral data.

The C−F in-plane bending modes have strong to medium intensity generally in the region 550−250 cm^{-1}[47]. In the present study, the strong bands at 580 and 490 cm^{-1} were assigned to the C−F in-plane bending of FMBN. The bands observed at 201 and 153 cm^{-1} were assigned to the C−F out-of-plane bending mode of FMBN.

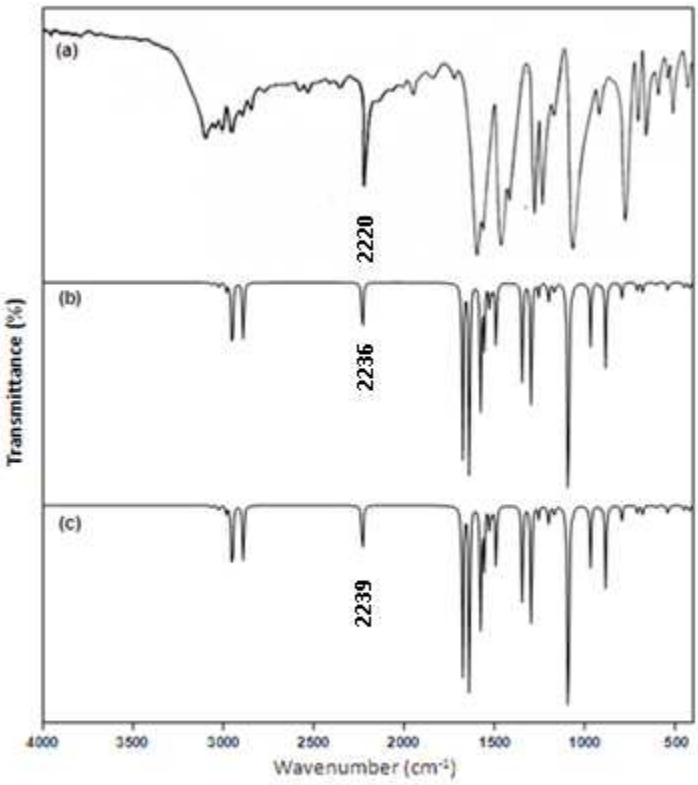

Fig. 2 FT-IR *spectrum* of 2-fluoro-6-methoxybenzonitrile
(a) Observed (b) HF/6-31G(d,p) (c) B3LYP/6-31G(d,p)

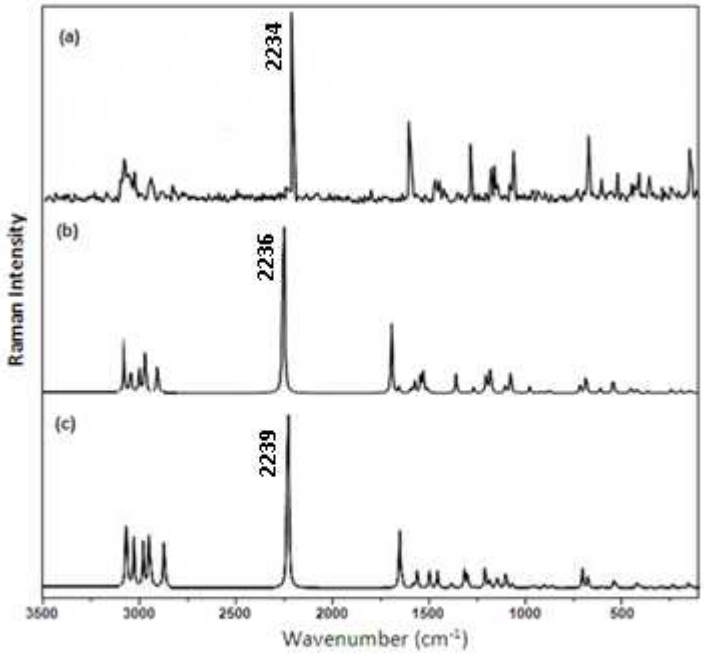

Fig. 3 FT-Raman *spectrum* of 2-fluoro-6-methoxybenzonitrile
(a) Observed (b) HF/6-31G(d,p) (c) B3LYP/6-31G(d,p)

HOMO-LUMO ANALYSIS

The Highest Occupied Molecular Orbital (HOMO) and Lowest Unoccupied Molecular Orbital (LUMO) are the main orbital that take part in chemical stability [48]. The HOMO represents the ability to donate an electron, whereas LUMO, as an electron acceptor, represents the ability to obtain an electron. The HOMO and LUMO

energies calculated by B3LYP/6-31G(d,p) method are as shown in Fig. 4. This electronic transition absorption corresponds to the transition from the ground to the first excited state and is mainly described by an electron excitation from the HOMO to LUMO. HOMO is located over the C−C; the HOMO-LUMO transition implies an electron density transfer to ring from C_l. Moreover, the orbital significantly overlaps in their position for FMBN. The calculated self-consistent field (SCF) energy of FMBN is (0.41884 a.u.)

OTHER MOLECULAR PROPERTIES

Thermodynamic Functions

Several calculated thermodynamic parameters are given in Table 6. Scale factors have been recommended [49] for an accurate predication in determining the zero-point vibration energies (ZPVE), and the entropy(S) vib(T) and they can be used with the values of this table. The changes in the total entropy of FMBN at room temperature at different methods are only marginal. The total energies and the change in the total entropy of FMBN at room temperature at different methods are also presented in Table 6.

Electrostatic Potential

Molecular Electrostatic Potential (ESP) at a point in the space around a molecule gives an indication of the net electrostatic effect produced at that point by the total charge distribution (electron + nuclei) of the molecule and correlates with dipole moments, electronegativity, partial charges and chemical reactivity of the molecules. It provides a visual method to understand the relative polarity of the molecule. An electron density isosurface mapped with electrostatic potential surface depicts the size, shape, charge density and site of chemical reactivity of the molecules.

The different values of the electrostatic potential represented by different colours; red represents the regions of the most negative electrostatic potential, blue represents the regions of the most positive electrostatic potential and green represents the region of zero potential. Potential increases in the order red < orange < yellow < green < blue. Such mapped electrostatic potential surfaces have been plotted for title molecule in B3LYP/6-31G(d,P) basis set using the computer software Gauss view. Projections of these surfaces along the molecular plane and a perpendicular plane are given in Fig. 5. This Fig provides a visual representation of the chemically active sites and comparative reactivity of atoms [48].

Table 6Thermodynamic functions of 2-fluro-6-methoxybenzonitrile obtained by HF and B3LYP level with the standard 6-31G(d,p) basis set.

Parameter	HF/6-31G(d,p)	B3LYP/6-31G(d,p)
Zero point vibrational energy(Kcal/mol)	83.0474	77.3203
Rotational constants (GHz)	1.47127	1.46262
	1.17390	1.15582
	0.68072	0.66959
Entropy (Cal/mol K)		
Total	95.075	98.216
Specific heat capacity at constant volume	33.163	35.560
Translational energy	88.811	83.479
Rotational energy	0.889	0.889
Vibrational energy	87.034	81.701
Dipole moment (D)	1.5748	1.3950

Natural bond orbital analysis

In the Table 7, BD(1) C2 – F9 orbital with 1.995 electrons has 27.87% C2 character in a sp3.35 hybrid and has 72.13% character in sp2.36 hybrid. The $sp^{3.35}$ hybrid on C2 has 76.78% p-character and the $sp^{2.36}$ hybrid on F9 has 70.22% p-character. The two coefficients 0.5279 and 0.8493 are called polarization. The size of these polarization coefficients shows the importance of the two hybrids in the formation of the bond. The fluorine has larger percentage of this NBO, gives the larger polarization coefficient of 0.8493 because it has higher electro negatively. At the end of the table fluorine and nitrogen lone pair NBO's are expected to be Lewis structure.

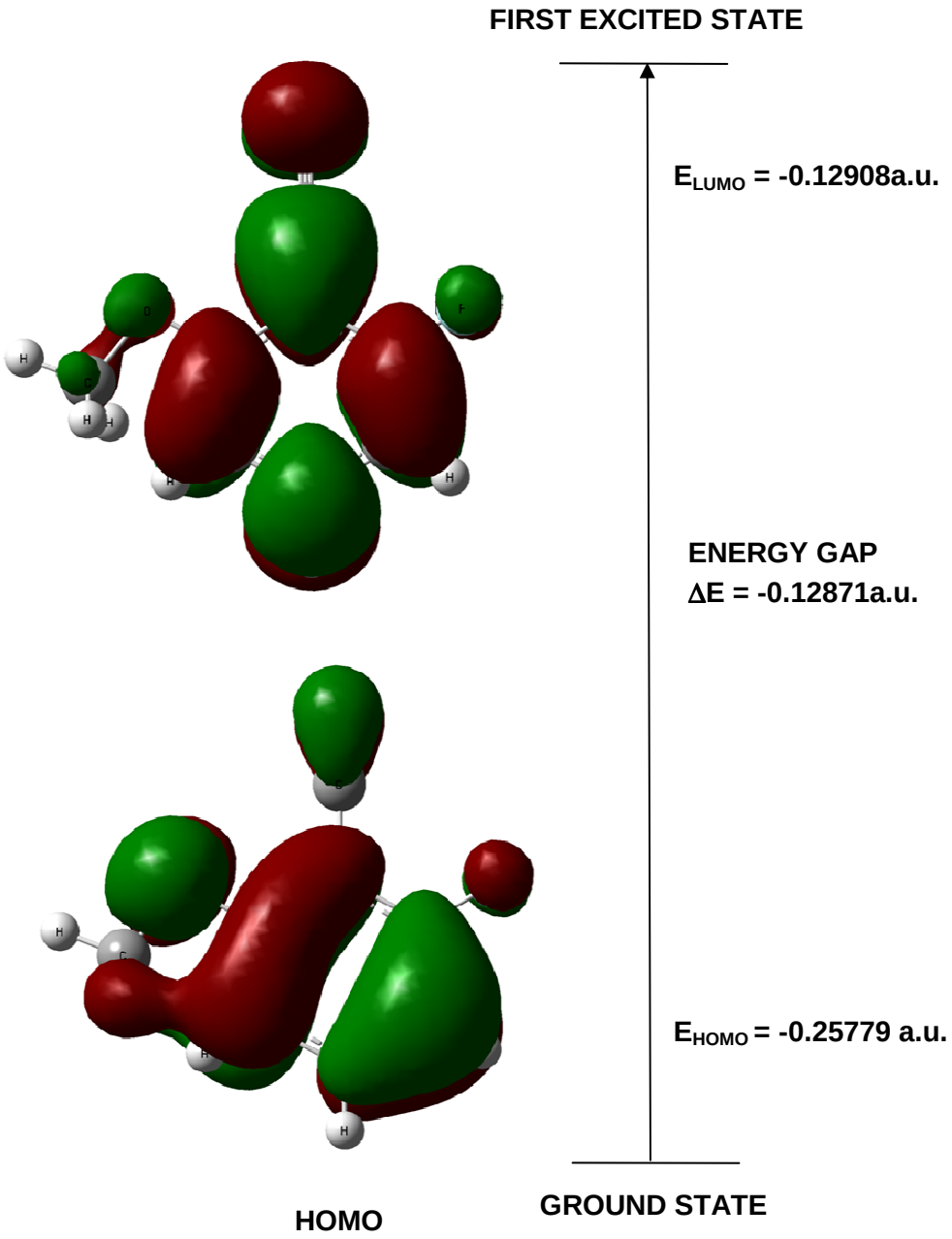

Fig. 4 HOMO-LUMO structure of 2-fluoro-6-methoxybenzonitrile

Second order perturbation theory analysis

Delocalization of the electron density between occupied (bond (or) lone pair) Lewis type NBO orbital's and formally unoccupied (antibond (or) Rydberge) non Lewis NBO orbital's corresponding to a stabilizing donor–acceptor interaction. These interactions can strengthen and weaken bonds. The energy of this interaction can be estimated by the second order perturbation theory [49]. The Table 8 lists the calculated second order interaction energies $E^{(2)}$ between the donor–acceptor orbital's in FMBN.

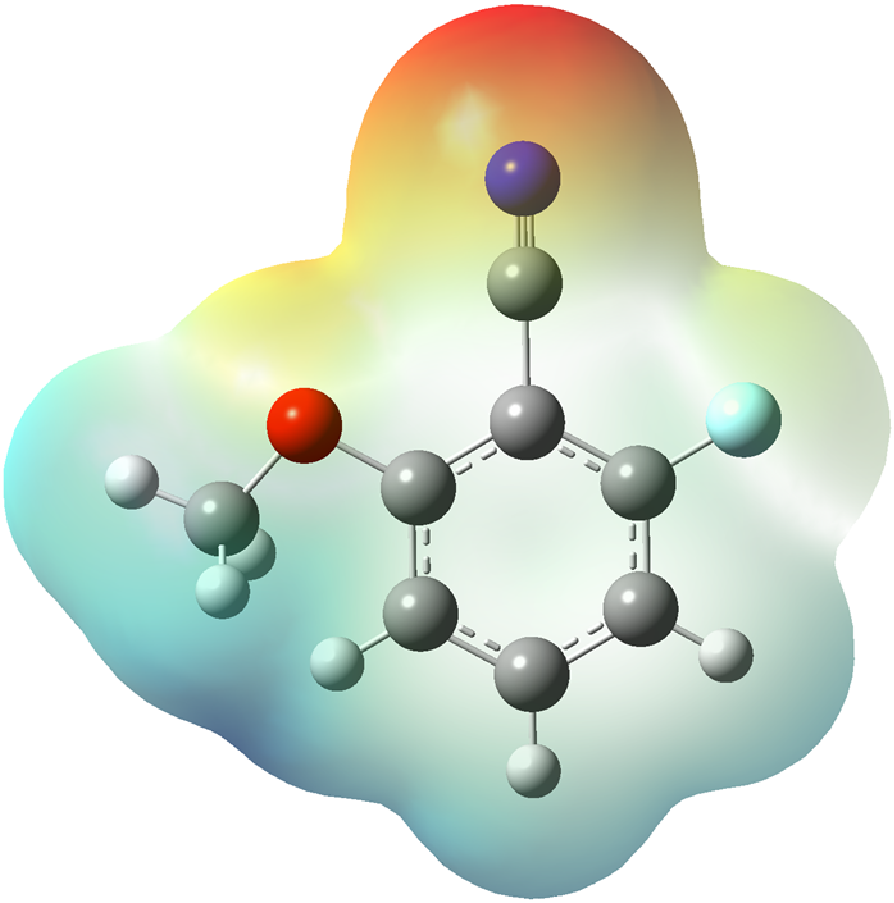

Fig. 5 Electrostatic potential surface of 2-fluoro-6-methoxybenzonitrile

Table 7 Natural bond orbital analysis of 2-fluoro-6-methoxybenzonitrile obtained by B3LYP/ 6-31G (d,p) level of theory.

Bond (A−B)	ED/energy (a.u)	ED_A (%) (a.u)	S (%)	P (%)	NBO	ED_B (%) (a.u)	S (%)	P (%)
BD(1) C1 - C 2	1.973	52.10	36.01	63.95	0.7218 ($SP^{1.78}$)C + 0.6921($SP^{1.64}$)C	47.90	37.83	62.13
BD(1) C1 - C6	1.971	51.91	37.31	62.66	0.7205($SP^{1.68}$)C +0.6935($SP^{1.7}$)C	48.09	36.98	62.98
BD(1) C1 - C7	1.980	50.90	26.65	73.31	0.7135($SP^{2.75}$)C +0.7007($SP^{0.93}$)C	49.10	51.87	48.09
BD(1) C2 - F9	1.995	27.87	22.92	76.78	0.5279($SP^{3.35}$)C +0.8493($SP^{2.36}$)F	72.13	29.70	70.22
BD(1) C3 - C4	1.976	50.34	35.61	64.36	0.7095($SP^{1.81}$)C +0.7047($SP^{1.9}$)C	49.66	34.53	65.43
BD(1) C4 - C5	1.976	49.80	34.81	65.15	0.7057($SP^{1.87}$)C +0.7085($SP^{1.85}$)C	50.20	35.08	64.88
BD(1) C5 - C6	1.979	49.81	34.43	65.53	0.7057($SP^{1.9}$)C +0.7085($SP^{1.62}$)C	50.19	38.20	61.76
LP (1) N8	1.967	-	36.01	-	$SP^{0.86}$	52.10	53.67	46.27
LP (1) F9	1.988	-	37.31	-	$SP^{0.42}$	51.91	70.29	29.71
LP (1)O13	1.950	-	35.61	-	$SP^{1.21}$	50.34	45.28	54.65
BD*(1) C1 - C2	0.035	47.90	34.43	63.95	0.6921($SP^{1.78}$)C +-0.7218($SP^{1.64}$)C	49.81	37.83	62.13
BD*(1) C1 - C6	0.034	48.09	36.01	62.66	0.6935($SP^{1.68}$)C +-0.7205($SP^{1.7}$)C	47.90	36.98	62.98
BD*(1) C1 - C7	0.033	49.10	37.31	73.31	0.7007($SP^{2.75}$)C +-0.7135($SP^{0.93}$)C	48.09	51.87	48.09
BD*(1) C2 - F9	0.027	72.13	26.65	76.78	0.8493($SP^{3.35}$)C +-0.5279($SP^{2.36}$)F	49.10	29.70	70.22
BD*(1) C3 - C4	0.015	49.66	22.92	64.36	0.7047($SP^{1.81}$)C +-0.7095($SP^{1.9}$)C	72.13	34.53	65.43
BD*(1) C4 - C5	0.015	50.20	35.61	65.15	0.7085($SP^{1.87}$)C +-0.7057($SP^{1.85}$)C	49.66	35.08	64.88
BD*(1) C5 - C6	0.027	50.19	34.81	65.53	0.7085($SP^{1.9}$)C +-0.7057($SP^{1.62}$)C	50.20	38.20	61.76

Table 8 Second order perturbation theory analysis of 2-Fluoro-6-methoxybenzonitrile at B3LYP/6-31G (d,p) basis set.

Donor (i)	Acceptor (j)	$E^{(2)}$ (kcal/mol)	E(j) – E(i) (a.u)	F(i,j) (a.u)
BD (1) C1 - C2	BD*(1) C1 - C6	3.89	1.3	0.063
BD (1) C1 - C2	BD*(1) C1 - C7	1.53	1.11	0.037
BD (1) C1 - C2	BD*(1) C2 - C3	2.9	1.29	0.055
BD (1) C1 - C2	BD*(1) C3 - H10	1.87	1.24	0.043
BD (1) C1 - C2	BD*(1) C6 - O13	3.73	1.03	0.055
BD (1) C1 - C2	BD*(1) C7 - N8	2.94	1.65	0.062
BD (1) C1 - C6	BD*(1) C1 - C2	3.75	1.28	0.062
BD (1) C1 - C6	BD*(1) C1 - C7	1.83	1.11	0.04
BD (1) C1 - C6	BD*(1) C2 - F 9	3.56	0.99	0.053
BD (1) C1 - C6	BD*(1) C5 - C6	2.96	1.3	0.055
BD (1) C1 - C6	BD*(1) C5 - H12	1.85	1.23	0.043
BD (1) C1 - C6	BD*(1) C7 - N8	3.09	1.64	0.064
BD (1) C1 - C7	BD*(1) C1 - C6	1.41	1.22	0.037
BD (1) C1 - C7	BD*(1) C2 - C3	2.63	1.21	0.05
BD (1) C1 - C7	BD*(1) C 5 - C6	2.84	1.23	0.053
BD (1) C1 - C7	BD*(1) C7 - N 8	2.92	1.57	0.061
BD (1) C2 - C3	BD*(1) C1 - C2	3.53	1.27	0.06
BD (1) C2 - C3	BD*(1) C1 - C7	3.57	1.1	0.056
BD (1) C2 - C3	BD*(1) C3 - C 4	2.16	1.29	0.047
BD (1) C2 - C3	BD*(1) C3 - H10	1.31	1.22	0.036
BD (1) C2 - C3	BD*(1) C4 - H11	2.07	1.22	0.045
BD (1) C2 - F 9	BD*(1) C1 - C6	1.55	1.57	0.044
BD (1) C2 - F 9	BD*(1) C3 - C 4	1.25	1.58	0.04
BD (1) C3 - C4	BD*(1) C2 - C3	2.1	1.25	0.046
BD (1) C3 - C4	BD*(1) C2 - F 9	4.29	0.97	0.057
BD (1) C3 - C4	BD*(1) C3 - H10	1.49	1.2	0.038
BD (1) C3 - C4	BD*(1) C4 - C 5	2.27	1.27	0.048
BD (1) C3 - C4	BD*(1) C4 - H11	1.16	1.21	0.033
BD (1) C3 - C4	BD*(1) C5 - H12	2.29	1.2	0.047
BD (1) C3 - H10	BD*(1) C1 - C2	4.14	1.08	0.06
LP (1) N8	BD*(1) C1 - C7	11.76	0.87	0.09
LP (1) F9	BD*(1) C1 - C2	1.41	1.58	0.042
LP (1) F9	BD*(1) C2 - C3	1.42	1.58	0.042
LP (1) O13	BD*(2) C1 - C 6	4.09	0.58	0.048
LP (1) O13	BD*(1) C5 - C 6	2.45	1.13	0.047
LP (1) O13	BD*(1) C14 - H16	1.25	1.08	0.033
LP (1) O13	BD*(1) C14 - H 17	1.26	1.06	0.033

The most important interaction energies are related to the resonance in the ring are electron donating from the BD (1) C1–C2, BD (1) C1–C2, BD (1) C1–C6, BD (1) C1–C6, BD (1) C2–C3, BD (1) C2–C3, BD (1) C3–C4, BD (1) C3–H10, LP (1) N8 to the anti-bonding acceptor BD*(1) C1–C6, BD*(1) C6 – O13, BD*(1) C1–C2, BD*(1) C2–F9, BD*(1) C1–C2, BD*(1) C1–C7, BD*(1) C2–F9, BD*(1) C1–C2, BD*(1) C1–C7 orbital's and their corresponding energies are 3.89, 3.73, 3.75, 3.56, 3.53, 3.57, 4.29, 4.14, 11.76 kcal/mol, respectively. These interactions clearly indicate the strongest stabilization energy increase of electron delocalization occurs due to substitution of the molecule.

CONCLUSION

The equilibrium geometries and the calculated frequencies of FMBN were determined and analyzed. The small distortions of the benzene ring are explained in terms of the change in hybridization affected by the substituent at the carbon site to which it is appended. The theoretically computed wavenumbers by B3LYP/6-31G (d,p) than HF/6-31G (d,p) level were found good agreement with experimental FT-IR and FT-Raman spectral data. The difference between the observed and theoretical values of most of the fundamentals is very small and therefore, the assignment seems to be correct. The electrostatic potential surfaces (ESP) together with complete analysis of the vibrational spectra, both FT – IR, FT – Raman and electronic spectra help to identify the structural and symmetry properties of the title molecule. NBO analysis provides an efficient method for studying inter and intra molecular interaction in molecular system. The stabilization energy has been calculated from second order perturbation theory. Natural Bond Orbital analysis shows the differences in interaction of energies are due to the substitution of CH_3 group, and electronegative atoms (nitrogen, fluorine), respectively.

REFERENCES

[1] V Krishnakumar; G Keresztury; T Sundius; R Ramaswamy, *J Mol. Struct*. **2004**, 702, 9–21.
[2] M A Palafox; V K Rastogi; L Mittal, *Int J Quantum Chem.* **2003**, 94, 189–204.
[3] H Irugartingev; E Fettle; T Eschev; P Tinneteld; S Nord; M Fauer, *Eur J. Org. Chem.* **2000,** 3 455–465.

[4] V K Rastogi; M A Palafox; R P Tanwar; Lalitmittal, *Spectrochim. Acta*, **2002**, 58 1987–2004.
[5] V Kumar; Y Panikar; M A Palafox; J K Vats; I Kostova; K Long; V Rastogi, *Indian J. Pure Appl. Phys.* **2010**, 48, 85–94.
[6] S Maiti ; A I Jaman ; A Datta ; R N Nandi, *J. Mol. Spectrosc*, **1990,** 140, 416–418.
[7] S D Sharma; S Doraiswamy, *J. Mol. Spectrosc*, **1996,** 180, 7–14.
[8] M A Palafox; V K Rastogi; J K Vats, *J. Raman Spectrosc.* **2006**, 37, 85–99.
[9] (a) A Joshi; K R Suryanarayana; M.A. Shashidhar, *Curr. Sci.* **1988**, 57, 477–478.
(b) V K Rastogi; V Jain; M A Palafox; D N Singh; R Yadav, *Spectrochim. Acta*, **2001,** 57, 209–216.
[10] M K Aralakkanavar; A M Joshi; R Rao; K R Suryanarayana; M A Shashidhar, *Indian J. Phys.* **1990,** 64, 152.
[11] S Mohan; R Murugan; S Srinivasan, *Proc. Natl. Acad. Sci. Ind. (Phys. Sci),* **1992**, 62, 121.
[12] R K Goel; S K Sharma; N Sharma, *Indian J. Pure Appl. Phys.* **1983**, 21 61.
[13] V K Rastogi; M A Palafox; S Chatar; R P Tanwar, *Spectrochim. Acta.* **2001,** 57, 2373–2389.
[14] V Mukherjee; N P Singh; R A Yadav, *Spectrochim. Acta*. **2011**, 81, 609–619.
[15] V K Rastogi; M A Palafox; S Singh; S K Singhal, *Asian J. Phys.* **1998,** 7, 229.
[16] W Koch; M C Colthausen, A. Chemist's Guide to Density Functional Theory, Wiley-VCH; Weinheim, New York, Chichester, **2000**.
[17] M Zheng; J Wang; J Zhang; S Luo, *Acta Cryst.* **2010,** 66, 1856–1864.
[18] M J Frisch; G W Trucks; H B Schlegel; G E Scuseria, et al., Gaussian 09, Revision A 02 (Inc., Wallingford CT) **2009**.
[19] R R Parr; R G Yang, Density Functional Theory of Atoms and Molecules. Oxford University Press; New York, USA, **1989**, and references therein.
[20] A D Becke, *J. Chem. Phys.* **1993,** 98, 5648–5652.
[21] C Lee; W Yang; R G Parr, *Phys. Rev. V*, **1988,** 37, 785–789.
[22] H Lampert; W Mikenda; A Karpten, *J. Phys. Chem.* **1997,** 101 2254-2263.
[23] T Sundius, Vibrational Spectrosc, 29 (2002) 89, MOLVIB, V.7.0, Calculations of Harmonic Force Fields and Vibrational modes of molecules, QCPE Program No. 807 **(2002**).
[24] P Pulay; G Fogarasi; J E Boggs; A Vargha, *J. Am. Chem. Soc.* **1983,** 105, 7037–7047.
[25] G Fogarasi; X Zhou; P W Taylor; P Pulay, *J. Am. Chem. Soc.* **1992**, 114 191–8201.
[26] A E Reed; F Weinhold, *J. Chem. Phys.* **1985,** 83, 1736–1740.
[27] A E Reed; R B Weinstock; F Weinhold, *J. Chem. Phys.* **1985**, 83, 735-746.
[28] A E Reed; F Weinhold, *J. Chem. Phys.* **1983**, 78, 4066–4073.
[29] J P Foster; F Weinhold, *J. Am. Chem. Soc.* **1980,** 102, 7211–7218.
[30] J Chocholousova; V Vladimir Spirko; P Hobza, *J. Phys. Chem. Chem. Phys*. **2004,** 6, 37–41.
[31] A Kovacs; I Hargittai, *Struc. Chem.* **2000**, 11 (2/3), 193–201.
[32] G Socrates, Infrared Characteristic Group Frequencies, John Wiley, New York, **1981**.
[33] P M Anbarasan; M K Subramanian; S Manimegala; K Suguna; V. Ilangovan; N Sundaraganesan, *J. Chem. Pharm. Res., **2011**, 3(3),123-136*.
[34] D Lin-Vien; N B Colthup; W G Fateley; J G Grasselli, The Handbook of Infrared and Raman Characteristics Frequencies of Organic Molecules, Academic Press, San Diego, CA, **1991**.
[35] J H S Green; D J Harrison, *Spectrochim. Acta*, **1976**, 32, 1279–1286.
[36] A P Kumar; G R Rao, *Spectrochim. Acta* **1997**, 2023–2033.
[37] J H S Green; D J Harrison, *Spectrochim. Acta* **1976,** 32, 1279.
[38] P S Kalsi, Spectroscopy of Organic Compounds, New Age International (P) Limited, Publishers, **2009**.
[39] P Udhayakala; T V Rajendiran; S Seshadri; S Gunasekaran, *J. Chem. Pharm. Res., **2011**, 3(3),610-625*.
[40] D Sajan; K P Laladhas; I Hubert Joe; V S Jayakumar, *J. Raman Spectrosc.* **2005,** 36, 1001–1011.
[41] L J Bellamy, The Infrared Spectra of Compound Molecules, Chapman and Hall, London, **1975**.
[42] N B Colthup; L H Daly; S E Wiberley, Introduction to Infrared and Raman Spectroscopy, Academic Press Inc., London, **1964**.
[43] S B Doddamani; A Ramoji; J Yenagi; J Tonannavar, *Spectrochim. Acta,* **2007**, 67 150–159.
[44] A M Huralikoppi, Investigation on the spectra of some substituted aromatic molecules; Ph. D thesis, Department of Physics, Karnataka University Dharrwad, 1995.
[45] S Muthu; E Isac Paulraj, *J. Chem. Pharm. Res., **2011**, 3(5),323-339.*
[46] V Krishnakumar; V Balachandran, *Spectrochim. Acta,* **2005,** 61 1001–1006.
[47] Priyanka Singh; N P Singh; R A Yadav, *J. Chem. Pharm. Res., **2011**, 3(1),737-755.*
[48] S Gunasekaran; R A Balaji; S Kumerasan; G Anand; S Srinivasan, *Can. J. Anal. Sci. Spectrosc.* **2008**, 53, 149.
[49] I Hubert Joe; I Kostova; C Ravikumar; M Amalanathan; S C Pinzaru, *J. Raman Spectrosc.* **2009,** 40, 1033–1038.